Title

THE COMPOSITION AND STRUCTURE OF OXIDE FILMS GROWN ON THE (110) CRYSTAL FACE OF IRON

Authors

Langell, M.
Somorjai, G.A.

Publication Date

1981-06-01

LBL-13203
Preprint

Lawrence Berkeley Laboratory
UNIVERSITY OF CALIFORNIA

Materials & Molecular Research Division

Submitted to the Journal of Vacuum Science and Technology

THE COMPOSITION AND STRUCTURE OF OXIDE FILMS GROWN ON THE (110) CRYSTAL FACE OF IRON

M. Langell and G.A. Somorjai

June 1981

Prepared for the U.S. Department of Energy under Contract W-7405-ENG-48

DISCLAIMER

THE COMPOSITION AND STRUCTURE OF OXIDE FILMS GROWN ON THE (110) CRYSTAL FACE OF IRON

M. Langell* and G. A. Somorjai

Materials and Molecular Research Division, Lawrence Berkeley Laboratory
and
Department of Chemistry, University of California, Berkeley, CA 94720

Abstract

Epitaxial oxide layers of Fe_3O_4-like composition and symmetry have grown on Fe(110) crystals exposed to oxygen gas. The epitaxial relationship between the oxide and the Fe(110) substrate is elucidated and the orientation of the oxide film has been explained in terms of the close registry between the Fe(110) and Fe_3O_4(111) crystal lattices. Both the structure and composition of the iron oxide epitaxies are a function of substrate temperature and oxygen pressure, and an oxide nucleation point has been observed over only part of the temperature-pressure range investigated. While oxide surfaces with Fe_2O_3-like composition have been observed, they are disordered and are only approximately one monolayer in thickness.

* Permanent Address: Department of Chemistry
University of Nebraska, Lincoln, NE 68588

This work was supported by the Director, Office of Energy Research, Office of Basic Energy Sciences, Materials Sciences Division of the U. S. Dept. of Energy under Contract W-7405-ENG-48

Introduction

The interaction of oxygen with iron leading to oxide formation is important in corrosion science and has, therefore, received much attention over the years. Recently, surface studies and studies analyzing the near-surface region have reported on the nature of the iron oxide formed under a range of oxidizing conditions. Below 500°C the predominant oxide detected on oxygen-exposed polycrystalline iron surfaces has been Fe_3O_4 with small amounts of δFe_2O_3 also present [1-5]. However, at least one study has reported the complete oxidation to αFe_2O_3 [6] under similar conditions. At higher temperatures [2,4] Fe_3O_4 has been observed exclusively. Although oxide species were detected early in the oxidation process, long exposures were necessary to achieve oxygen saturation and complete oxidation.

Oxidation of roughened foil samples [4] at 25-800°C under 10^{-6} to 10^{-3} torr O_2 showed preferential nucleation and epitaxial growth of the oxide with domains of (110). Low energy electron diffraction (LEED) studies [5] of air-exposed iron indicated that epitaxial oxide growth is also possible on single crystals, although small oxide crystallites and extensive faceting were observed. Electrochemical analysis identified the composition of these oriented oxide layers as Fe_3O_4 and δFe_2O_3. Use of more gentle conditions (123-473 K and 5×10^{-7} torr O_2)[7] on Fe(100) resulted in a more highly ordered oxide overlayer of approximately four layers thickness with FeO-like geometry. The predominant oxidation state of iron in these films was found to be Fe^{3+}.

The above studies cover a wide range of temperatures and pressures. However, no serious attempt has been made to correlate reaction conditions to the composition and structure of the oxide formed. In many cases the

oxygen pressure appears to have been arbitrarily chosen. We present here a systematic investigation of oxide films grown epitaxially on Fe(110) as a function of temperature in the range of 25 to 500°C and pressure at $5x10^{-8}$ to $5x10^{-6}$ torr O_2.

Experimental

The experiment was carried out in a Model 545 Physical Electronics system equippped with a single pass CMA Auger spectrometer and modified to include Varian four-grid retarding field optics for LEED analysis, a UTI quadrupole mass spectrometer and argon ion bombardment capabilities. In addition, the UHV chamber was fitted with a high pressure cell enabling the sample to be treated at pressures up to 1 atm. without exposing it to ambient atmospheric gases or compromising the ultrahigh vacuum [8]. Base pressure, typically in the range of $5x10^{-10}$ torr, was maintained by a 200 L sec ion pump with auxiliary pumping by titanium gettering and liquid nitrogen cryopumping.

Iron single crystal rod, supplied by Materials Research Corporation, was oriented to within 0.5° of the (110) plane, cut to a thickness of about 1 mm and polished to .05 microns Al_2O_3 paste before being introduced into the UHV chamber. Because of the reactivity of iron, removing trace impurities was time consuming. The impurities most notably were sulfur, oxygen, and nitrogen. The contaminants were reduced to a manageable level by argon ion sputtering at 600°C for a total of approximately 24 hours. At this point, nitrogen proved to be most troublesome.

Although the nitrogen was present in relatively small quantities, estimated at .05 to .1 monolayers (ML) by AES peak-to-peak intensities, it had a marked effect on the structure of the Fe(110) surface. The LEED pattern (Fig.1) showed

a complicated structure identified by Bozso et al.[9] as the reconstructed Fe_4N analog. The structure appeared here at lower surface concentrations than the .25 ML reported by Bozso as necessary for surface Fe_4N formation. However, the onset of reconstruction is dependent upon the amount of subsurface nitrogen which is believed to be higher in the present case involving surface segretation. Bozso's case resulted from the adsorption of N_2 and subsequent nitride formation.

Even small amounts of nitrogen on the surface of Fe(110) drastically reduce the stickig coefficient of O_2. For surfaces showing the LEED pattern of Fig. 1, and about .1 ML nitrogen, the initial sticking coefficient was reduced to one tenth that of the clean unreconstructed surface.

When the bulk concentration of nitrogen was finally depleted, the Fe(110) (1x1) LEED pattern was obtained (Fig. 2). The surface was then exposed to oxygen gas at $5x10^{-8}$ to $5x10^{-6}$ torr with iron surface temperatures of 25 to 500°C. Oxidation at each temperature-pressure combination was always begun on Fe(110) exhibiting the (1x1) clean surface LEED pattern and no impurities detectable by Auger electron spectroscopy (AES).

Results

1. Calibration of Auger peak intensities to determine oxide stoichiometry.

AES studies were carried out with iron oxide samples that served as reference to provide a calibration for Auger intensities for oxide overlayers. The oxides were Fe_3O_4 and α Fe_2O_3 samples that yield O/Fe Auger peak ratios of 3.7 ± .1 and 4.0 ± .1, respectively. The ratios were measured as peak-to-peak values of theoxygen KL_2L_2 transition at 510 eV to iron $L_3M_{2,3}M_{4,5}$ transition at 652 eV. These values are consistantly obtained, regardless of the means of preparation of the bulk oxide, as shown in Table I.

For bulk αFe_2O_3 samples with both O/Fe of 4.1 and 3.7 were observed. Surfaces with the two oxygen concentrations could be interconverted by subjecting the samples to oxidizing and reducing conditions. If reducing conditions became too severe, for example UHV conditions at >500°C, conversion to bulk Fe_3O_4 was observed as was indicated by the red to black color change of the sample. Fe_3O_4 surfaces on either samples obtained by the reduction of Fe_2O_3 or from pressed powdered samples of bulk Fe_3O_4 gave an Auger peak intensity ratio (O/Fe)=3.7, exclusively. This value could not be increased to 4.0 by exposure to oxygen without also converting the bulk to Fe_2O_3.

A logical assignment of the O/Fe Auger peak ratios is to associate the value of 4.1 with an αFe_2O_3-like surface composition and that of 3.7 with a Fe_3O_4-like composition. While Auger peak shapes are not expected to remain unaltered as a function of surface oxidation, the greatest change in the iron Auger spectrum takes place at the earlier stages of oxidation. Therefore, it is not surprising that the increase in O/Fe of 3.7 to 4.0 is almost in direct proportion to the increase in oxygen content in going from Fe_3O_4 to Fe_2O_3. First derivative peak-to-peak heights can therefore be used as a direct measurement of oxygen concentration in this range.

2. Oxidation of Fe(110) single crystal surfaces.

The Fe(110) that was clean as indicated by AES (Fig. 3) and ordered as indicated by LEED (Fig. 2), was exposed to oxygen at pressures of $5x10^{-8}$ torr to $5x10^{-6}$ torr and substrate tempeatures of 25 to 500°C. Although initial oxygen uptake was moderately rapid, the adsorption rate diminished due to decreasing sticking probability after ~ 150 L. Long exposures were therefore needed to saturate the near surface region with oxygen. At 200°C and $5x10^{-7}$ torr O_2, 1350 L exposure was required to achieve saturation.

Typical adsorption curves are shown in Fig. 4 for oxygen pressures of $5x10^{-7}$ torr. Here we plot the oxygen Auger peak intensity at 510 eV as a function of time at different crystal tempeatures. Thee regions can be distinguished in this temperature range of 100-500°C. At low temperatures, T<100°C, oxygen adsorption proceeds at a moderate rate until O/Fe values of ~ 1.7 are obtained. Depending on the oxygen pressure, the adsorption rate falls to zero for exposures of up to 1440 L (at $5x10^{-8}$ torr O_2) or takes place at a greatly reduced rate to saturate at (O/Fe)=3.4. The LEED surface structure is (1x1) at (O/Fe)=1.7, consistent with oxygen monolayer formation [10-12]. At (O/Fe)=3.4 there appears a more complicated LEED surface structure that will be discussed below.

At temperatures between 200 and 300°C the oxygen Auger peak intensity rises faster initially then appears to slow down until a point that will be referred to as the "oxide nucleation point" is reached at 360 L. Adsorption then proceeds at an increased rate to form an oxide with O/Fe of 3.7 and a surface structure of hexagonal symmetry (Fig. 6). Further oxygen exposure disorders this structure and the oxygen surface concentration saturates at (O/Fe)=4.0. The hexagonal surface structure can be regenerated by briefly flashing the crystal in vacuum to 500°C. The oxygen-to-iron Auger peak ratio of 3.7 is then recovered.

At temperatures above 400°C, no nucleation point is reached and a gradual saturation at (O/Fe)=1.7 is observed. The LEED pattern is a "reconstructed" hexagon (Fig. 7), to be described later. If the temperature is reduced to 300°C and oxygen exposure continued, the oxygen surface concentration increases to give (O/Fe) of 3.7 and the hexagonal surface structure devoid of reconstruction.

The effect of temperature and pressure on the structure and composition of the oxide epitaxy is summarized in Table II. The oxygen surface concentration

and thus the (O/Fe) Auger peak ratio is a function of both oxygen pressure and temperature; it increases with increasing oxygen pressure and decreasing temperatures. Thus the effect of raising the oxygen pressure from 400°C $5x10^{-7}$ torr to $5x10^{-6}$ torr at 400°C can also be created at constant pressure of $5x10^{-7}$ torr by lowering the oxidation temperature from 400°C to 300°C. Increasing the pressure from $5x10^{-8}$ to $5x10^{-7}$ torr at 100°C also increases the amount of oxygen that the sample is able to adsorb from (O/Fe)=1.7 to 3.4, and changes the surface structure from a simple (1x1) overlayer to the hexagonal ordered oxide.

3. $M_{2,3}VV$ iron valence structure

The greatest changes in iron Auger peak shapes occur during the initial stages of oxidation. These changes include broadening of the iron peaks, most noticeable in the 598, 652, and 703 eV transitions. The peak shape of the oxygen 510 eV Auger transition remains relatively unchanged. Unlike the higher energy iron Auger peaks, the $M_{2,3}$ VV at 47 eV exhibits changes over the entire oxygen adsorption region. Initially there is a large reduction in intensity and the appearance of a shoulder at 55 eV. Fig. 5a shows this transition after adsorption of about one monolayer of oxygen.

As oxygen adsorption continues, the $M_{2,3}$ VV transition shifts from 47 to 49 eV, obscuring the 55 eV peak. A new peak at 42 eV also emerges (Fig. 5b) and grows in intensity with further oxygen adsorption.

Ertl and Wandelt [1] have also reported a similar splitting of the $M_{2,3}$ VV transition for oxidized iron with surface composition of Fe_3O_4. With assistance of literature XPS and UPS data [13], the 47 eV peak can be correlated with valence states in the iron 3d bands and the lower energy peak with the creation of a new valence band by admixture with oxygen 2p electrons.

4. LEED studies

LEED analysis indicated the growth of an ordered oxide film on the Fe(110) substrate. The surface oxides have hexagonal symmetry, the simplest structure being that shown in Fig. 6. The broad diffraction spots indicate the presence of small, relatively well ordered domains with diameters of only ~ 40 Å [14]. The domain size did not change perceptively with oxide film thickness, nor is the ordering improved with short annealing to temperatures as high as 600°C.

The hexagonal LEED pattern was observed for all films under the conditions of (O/Fe)=3.7 that corresponds to oxygen concentration comparable to that observed on Fe_3O_4 standards. Attempts to further adsorb oxygen on the hexagonal Fe_3O_4-like surface produced only disordered adsorption. While it was possible to increase the oxygen Auger signal to (O/Fe)=4.0, as observed for bulk Fe_2O_3 samples, the excess oxygen was easily removed by flashing the sample to 350°C under UHV conditions and is therefore considered to be produced only at the outermost layers of the oxide film. The hexagonal LEED pattern that was regenerated upon flashing had the O/Fe Auger ratio again indicating Fe_3O_4-like composition. The hexagonal surface structure was also observed on saturated surfaces when the oxygen-to-iron Auger peak ratio was as low as 3.4, 8% lower than for Fe_3O_4.

The 'reconstructed' structure is also of hexagonal symmetry (Fig. 7) and is similar to the structure of reconstructed Fe(110) surfaces such as Fe(100)-C and Fe(110)-N, if variations in fractional order beam intensities are taken into account. The 'circular' Fe(110) carbon-contaminated structure and the iron nitride pattern mentioned earlier have been described in terms of reconstruction of the Fe(110) lattice. One possible assignment discussed by Bozso et al. [9] is shown in Fig. 8 for the reconstructed iron lattice.

The reconstructed surface could easily be converted to the (1x1) hexagonal structure by either lowering the temperature or increasing the pressure. However, the reverse transformation from hexagonal to reconstructed hexagonal surface structure was not possible. Heating the hexagonal surface under UHV at 600°C for periods of several hours caused iron migration into the oxide region and thus a lowering of oxygen concentration. The resulting LEED pattern was a combination of Fe(110) and hexagonal Fe_3O_4 oxide structures and was first observed for O/Fe Auger intensity ratios below 2.3, about 40% depleted from the saturated Fe_3O_4-like hexagonal surace.

The hexagonal surface structure of the oxide can easily be rationalized from the bulk symmetry of Fe_3O_4 (Fig. 9a). The Fe_3O_4 framework consists of a cubic close packed oxygen network and thus gives a basal plane of hexagonal symmetry. The filling of iron sites, 1/2 the possible octahedral and 1/8 the tetrahedral sites, presents more of a problem. If the sites are occupied in an ordered manner, the symmetry of the resulting structure will be lowered and fractional order diffraction features should be observed. Since no fractional beams are observed from the saturated Fe_3O_4-like epitaxy, it is suggested that a random filling of iron sites takes place.

It is also possible to obtain a structure with hexagonal symetry and correct dimensions by considering a defect-ridden αFe_2O_3 corrundum structure formed of hexagonal close packed oxygen with 2/3 of the octahedral sites occupied in a pseudo-hexagonal manner (Fig. 9b). Again, a random arrangement of vacancies is required if no additional diffraction featues are to be expected in the LEED spectrum. The basic difference bewteen a vacancy-containing corrundum-like arangement and that of the Fe_3O_4 structure for the oxide films is the filling of additional octahedral sites at the expense of tetrahedral positions in the spinel structure. However, if only octahedral positions

need be considered, it is difficult to explain why further oxidation to Fe_2O_3-like composition is not observed.

Figure 10 shows the relationship between the Fe(110) substrate and the basal plane of bulk Fe_3O_4. A good coincidence occurs along the [001] direction with mismatch of only 3.5%. Analysis of the LEED pattern indicates that oxide epitaxy on the bulk Fe(110) substrate does indeed occur. The repeat distance in the surface oxide is compressed to 2.82 Å from 2.97 Å of the bulk oxide a value that is the same within experimental accuracy as the iron substrate spacing of 2.87 Å .

Discussion

The epitaxial oxide layer grown on Fe(110) single crystals is closely analogous to that of bulk magnetite, Fe_3O_4, in both structure and composition. The sequence for three dimensional oxide formation follows the pattern of (1) dissociative oxygen adsorption until 1 ML coverage is reached, (2) a slower oxygen uptake involving some oxygen penetration into the bulk until (3) oxide nucleation and more rapid oxygen uptake to saturation at the Fe_3O_4 oxide composition. The extent to which a single crystal iron surface oxidizes is dependent upon both temperature and pressure. At room temperature and in the range of 10^{-8} to 10^{-6} torr, only the first step, monolayer adsorption , is observed. This region has been studied extensively and the analysis of the Fe(110)-O submonolayer and monolayer structures is well documented in the literature [9-11].

Adsorption on the monolayer surface is initially sluggish from ~ 100 to 450 L of oxygen exposure. To proceed with oxygen uptake past the monolayer region, crystal temperatures of 100°C or greater are required. Argon ion sputtering at this stage of oxidation indicates significant oxygen penetration

into the bulk crystal. Thus the elevated temperature appears to be necessary to insure sufficient ion mobility to allow detectable rates of oxidation. Independent studies [15] have shown that the actual mechanism for iron oxidation involves iron migration outward through the oxide layer with subsequent reaction with oxygen at the interface.

Oxygen concetration in the chemisorption region saturates at the (O/Fe) Auger peak ratio of 1.7. After exposure to 450 L, nucleation of Fe_3O_4-like oxide takes place and is signaled by the sudden increase in the rate of oxygen adsorption. The point at which nucleation occurs is strongly dependent upon the oxidation conditions. Further oxygen exposure increases the thickness of the oxide layer without changing the oxygen concentration in regions for which the surface is saturated at (O/Fe) of 1.7. If the temperature is lowered, oxide nucleation immediately takes place and oxidation proceeds normally to produce the Fe_3O_4 hexagonal surface. Once formed, the Fe_3O_4 layers are stable, and to bring about its decomposition is difficult.

Under the entire temperature-pressure ranges investigated here, αFe_2O_3 is thermodynamically the most stable bulk oxide [16] and would be expected to form in the bulk during complete oxidation of the metal. Below 100°C for Fe(110) single crystals, iron mobility is insufficient to allow for multilayer oxide formation. Above this temperature, however, Fe_3O_4 appears to be the stable surface oxide. Several studies on bulk α Fe_2O_3 samples [1-7] have contended the surface composition to be largely of Fe_3O_4. Powdered and single crystal α Fe_2O_3 oxides, used as standards for Auger analysis in this study, also showed evidence for an Fe_3O_4 surface layer. Depending upon the sample treatment, however, Fe_2O_3-like surface composition was also obtained.

The hexagonal surface structure of the Fe_3O_4 close packing oxygen array

is well matched along the [001] direction of the Fe(110) surface and only 3.5% deviation in spacing is expected from simple bulk coincidence. The hexagonal oxide structure does indeed appear to have aligned with the Fe(110) substrate, decreasing the O-O distance from 2.97 Å of the bulk oxide to 2.82 Å in the oxide epitaxy. The distance between iron atoms along [001] in the Fe(110) surface is 2.866 Å .

Epitaxial growth of compounds during the oxidation of transition metals often results in epitaxial oxide overlayers. Several cases of epitaxial oxide growth are summarized in Table 3. The compound overlayer orientation is not necessarily the preferred growth plane of the bulk compound, but is that which is in closest coincidence with the transition metal substrate. An example is the WO_3(111) over layer which forms readily on W(110). Reconstruction of the metal, as during molybdenum oxidation to form MoO_2(110) on a Mo(110) surface reconstructed to the (112) orientation, is also observed. Finally, compounds can be stabilized on transition metal substrates to give epitaxies that otherwise would not form under the growth conditions, as is the case of Fe(100)-Fe_4N(002). The compound that forms on epitaxial growth therefore cannot be predicted entirely on the basis of bulk compound thermodynamics. One must also consider the interface structure with the transition metal substrate.

These considerations could explain the ease with which the Fe(100) surface oxidizes and grows multilayer epitaxies as compared to the sluggish behavior of the Fe(100) surface [12]. The Fe(100) surface will grow three to four layers of oxide with FeO-like geometry. The exact arrangement of the iron within the oxide layer is uncertain, but there is a considerable Fe^{3+} concentration in the epitaxial layer, suggesting a substantial number of iron vacancies. The exact stoichiometry of the Fe(100)-oxide was not determined, but with

larger amounts of Fe^{3+} present, a surface with concentrations similar to Fe_3O_4 or Fe_2O_3 is probable. Unlike the Fe(110)-oxide system, however, Fe(100) has no close epitaxial alignment with either Fe_2O_3 or Fe_3O_4 crystal structures and interfacing of an oxide face with the Fe(100) surface is more difficult.

Conclusion

The iron oxide structure and composition that grows epitaxially on Fe(100) is sensitive to both temperature and pressure. Temepratures of ~ 100°C are needed for three-dimensional oxidation to allows for sufficient iron mobility. Under ideal conditions, an Fe_3O_4-like oxide forms with hexagonal symmetry that is in close registry with that of the Fe(110) substrate. The oxide maintains its surface structure for thickness greater than 40 Å with no visible degradation of the LEED pattern. At higher temperatures (>400°C at 5×10^{-6} torr) the oxide is not able to nucleate and a lower concentration, approximately Fe_7O_{10}, is obtained. This surface will readily nucleate Fe_3O_4 species if the temperature is lowered to the correct range for nucleation.

Acknowledgment

This work was supported by the Director, Office of Energy Research, Office of Basic Energy Sciences, Materials Sciences Division of the U.S. Department of Energy under Contract W-7405-ENG-48.

References

1. G. Ertl and K. Wandelt, Surf. Sci. 50 (175) 479.

2. J.H.W. DeWit, A.F. Broersma, and M. Strobard, J. Solid State Chem. 37, (1981) 242.

3. K. Haneda and A.H. Morrish, Surf. Sci. 77 (1978) 584.

4. G.K.L. Cranstoun and J.T. Lynch, Appl. Surf. Sci. 5 (1980) 161.

5. P.B. Sewell, C.D. Stockbridge, and M. Cohen. J. Electrochem. Soc. 108 (1961) 933.

6. J.K. Gimjewski, B.D. Padalia, S. Affrossman, L.M. Watson, and D.J. Fabian, Surf. Sci. 62 (1977) 386)

7. C.R. Brundle, IBM J. Res. Deelop. 22 (1978) 235.

8. D.W. Blakely, E. Kozak, B.A. Sexton, and G.A. Somorjai, J. Vac. Sci. & Technol. 13 (1976) 1019.

9. F. Bozso, G. Ertl. and M. Weiss, J. Catal. 50 (1977) 519.

10. C. Leygraf and S. Ekelund, Surf. Sci. 40 (1973) 609.

11. A.J. Melmed and J.J. Carroll, J. Vac. Sci. Technol. 10 (1973) 164.

12. C.R. Brundle, Surf. Sci. 66 (1977) 581.

13. S.G. Bishop and P. C. Kemeny, Solid State Commun. 15 (1974) 1877.

14. G. Ertl and J. Kuppers, Low Energy Electron Diffraction, Verlag Chemie, Weinheim, Germany, 1974.

15. L.S. Darken and R.W. Gurry, Physical Chemistry of Metals, McGraw Hill, New York, 1953.

16. F.A. Cotton and G. Wilkenson, Advanced Inorganic Chemistry, 3rd Ed., Interscience Publishers, New York, 1972, p.888.

17. H.M. Kennett and A.E. Lee, Surf. Sci. 48 (1975) 591, 606, 617, 624, 633.

18. J.C. Tracy and J.M. Blakely, Surf. Sci. 13 (1968) 313.

19. N.R.Avery, Surf. Sci. 41 (1974) 533.

20. F. Bozso, G. Ertl, M. Grunze, and M. Weiss, J. Catal. 49 (1977) 18.

Figure Captions

Fig. 1 Fe(110)-nitride pattern at (a) 65 eV and (b) 80 eV.

Fig. 2 Fe(110) clean surface (1x1) at (a) 100 eV and (b) 250 eV.

Fig. 3 Clean Fe(100) Auger spectrum. Conditions are 2.0 keV primary energy, 3.5 μ amps beam current, 2 eV modulation energy, 5 eV/sec sweep time, and .1 sec time constant.

Fig. 4 Adsorption isotherms for oxygen at $5x10^{-7}$ torr and temperatures of 100 to 500°C as measured by the peak-to-peak intensity of the oxygen KLL Auger transition.

Fig. 5 $M_{2,3}$ VV iron valence structure (a) 1 monolayer oxygen coverage, (b) saturated Fe(110)-oxide with O/Fe of 3.7, (c) bulk α Fe_2O_3 oxide from single crystal with O/Fe of 3.71.

Fig. 6 Hexagonal oxide structure observed in regions one and two (a) 80 eV and (b) 125 eV.

Fig. 7 Reconstructed iron oxide epitaxy formed at $5x10^{-7}$ torr and 400°C (a) 80 eV, and (b) 100 eV.

Fig. 8 Reconstruction of Fe(110) as proposed in Ref. 9. Only the position of the iron atoms are indicated.

Fig. 9 Symmetry of bulk iron oxides (a) Fe_3O_4 spinel basal plane, (b) α Fe_2O_3 corrundum basal plane.

Fig. 10 Coincidence between the Fe(110) surface and the oxygen positions of Fe_3O_4 basal plane, Note that along [001] the mismatch is only 3.5%.

Table Captions

Table 1. Bulk oxide Auger Ratios.

Table 2. Iron oxide epitaxies as a function of temperature and pressure.

Table 3. Metal-metal oxide epitaxial arrangement for some known surface compounds.

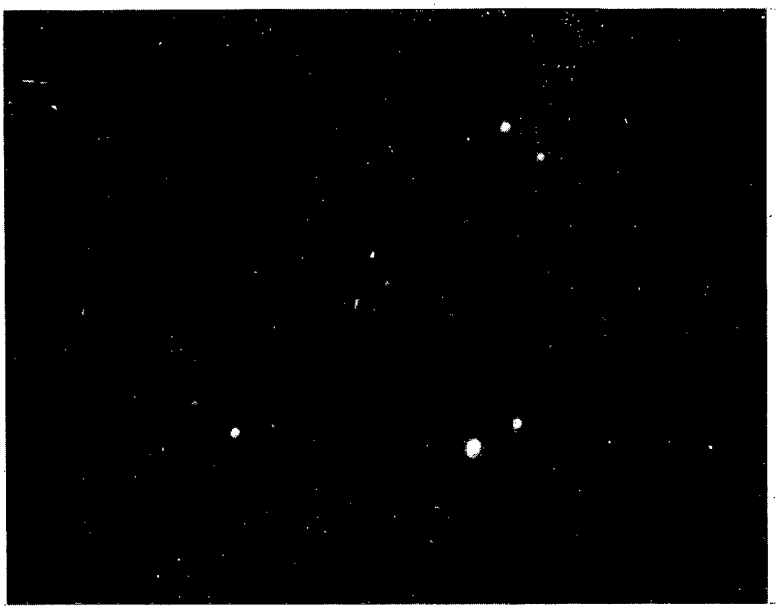

a

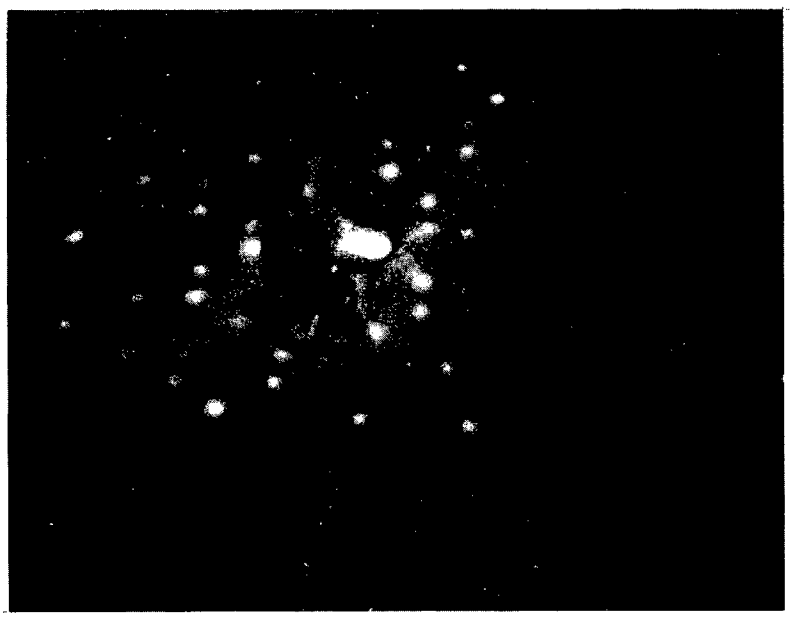

XBB 810-10161

b

Fig.1

a

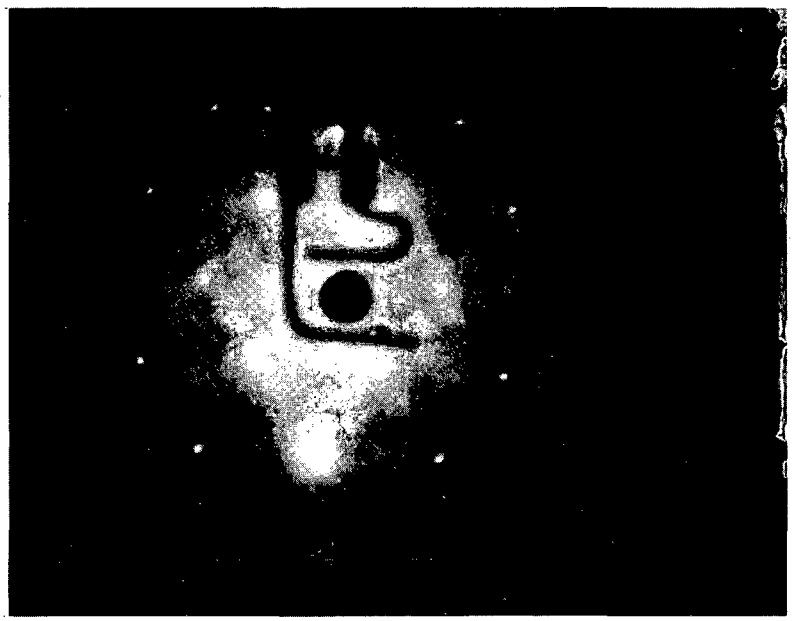

XBB 810-10162

b

Fig.2

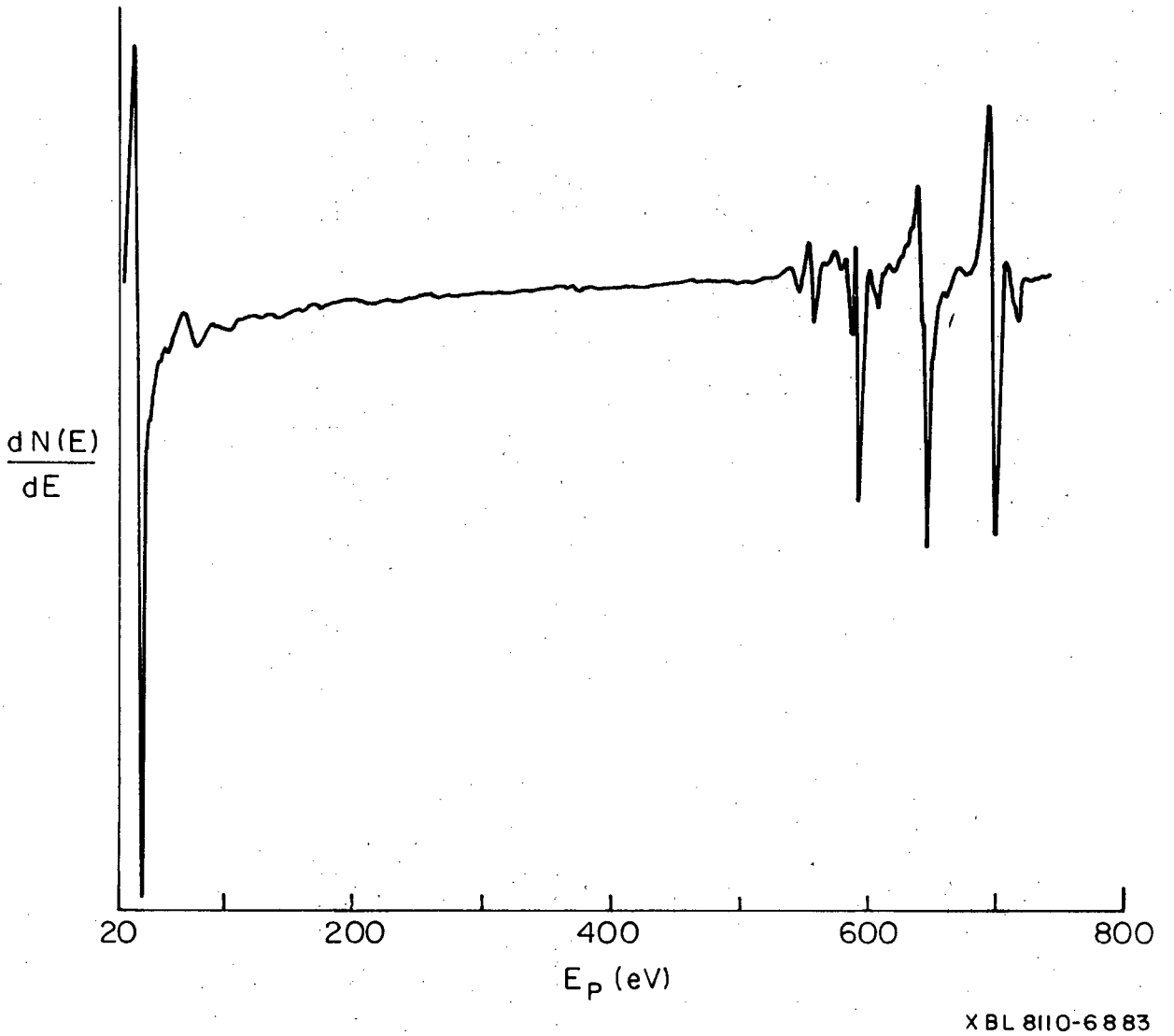

Fig.3

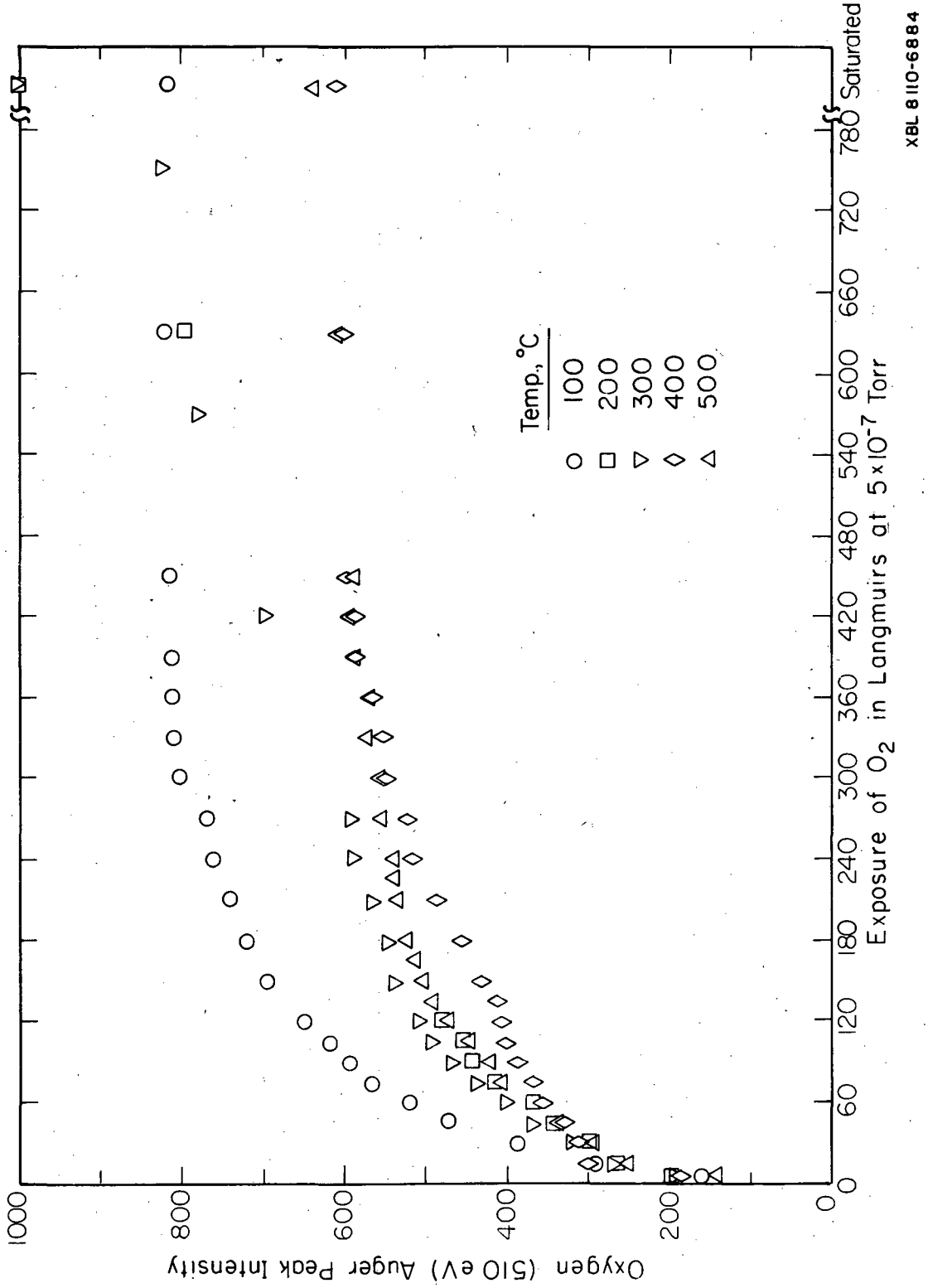
Oxygen (510 eV) Auger Peak Intensity
0
200
400
600
800
1000
0
60
120
180
240
300
360
420
480
540
600
660
720
780 Saturated
Exposure of O_2 in Langmuirs at 5×10^{-7} Torr
Temp., °C
100
200
300
400
500
XBL 8110-6884

Fig.4

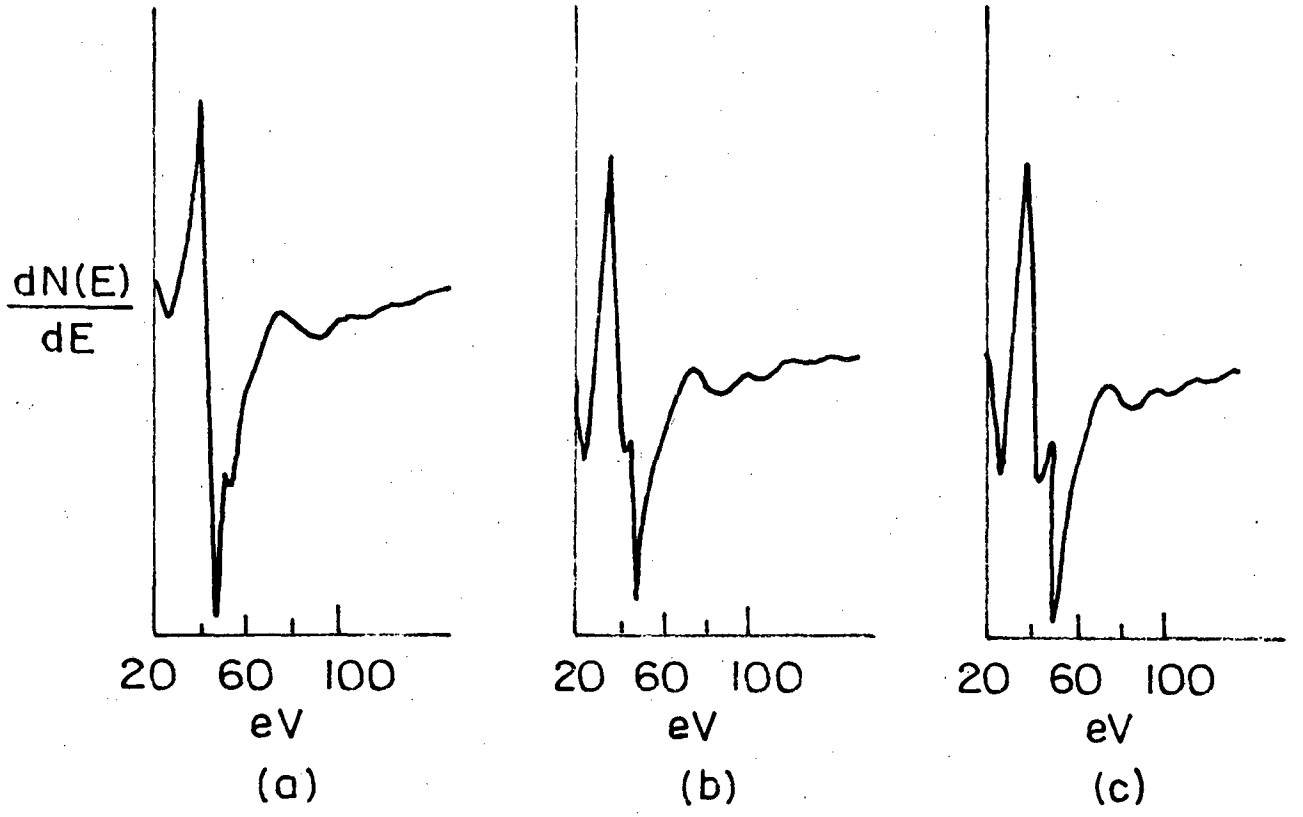

Fig.5

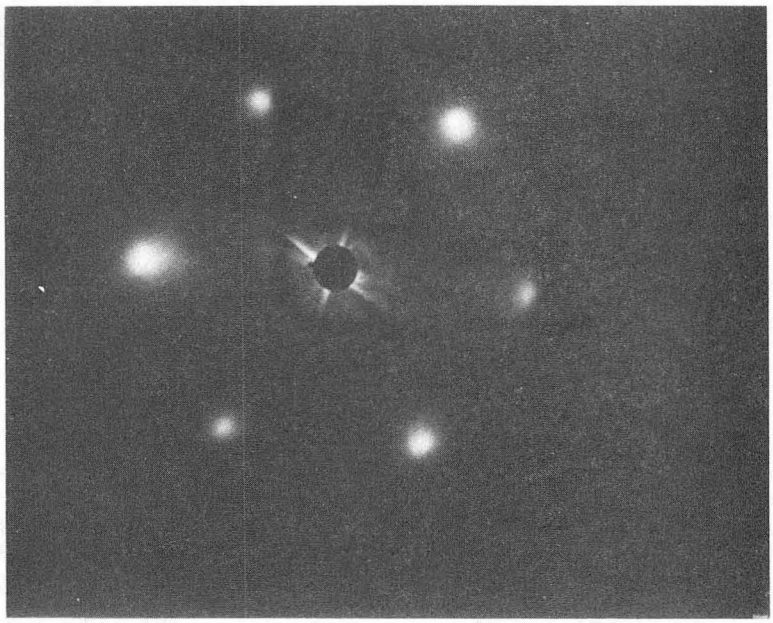

a

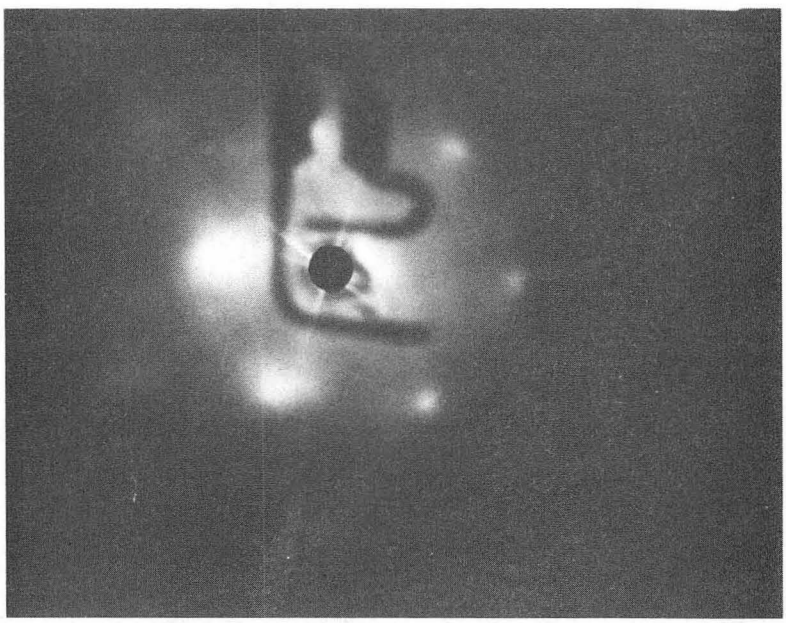

XBB 810-10163

b

Fig.6

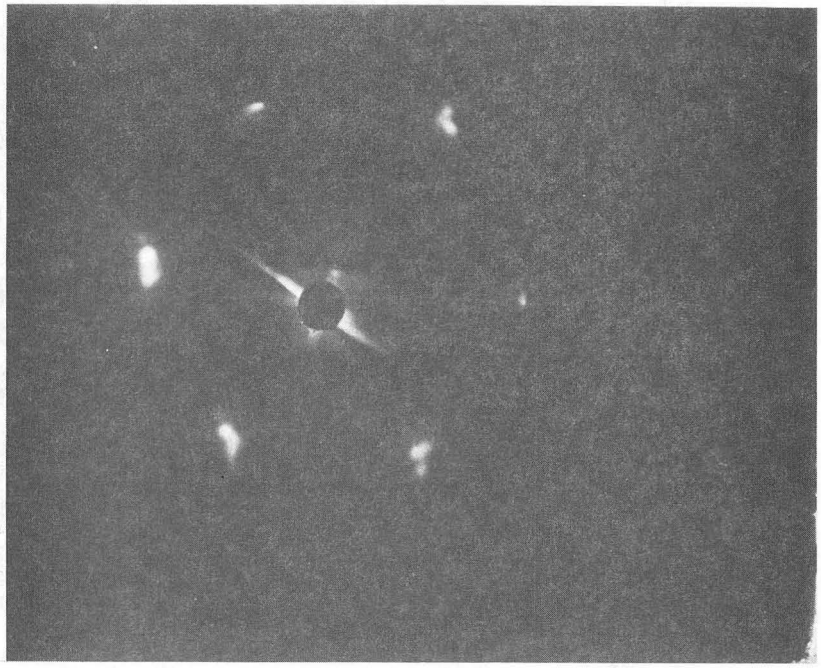

a

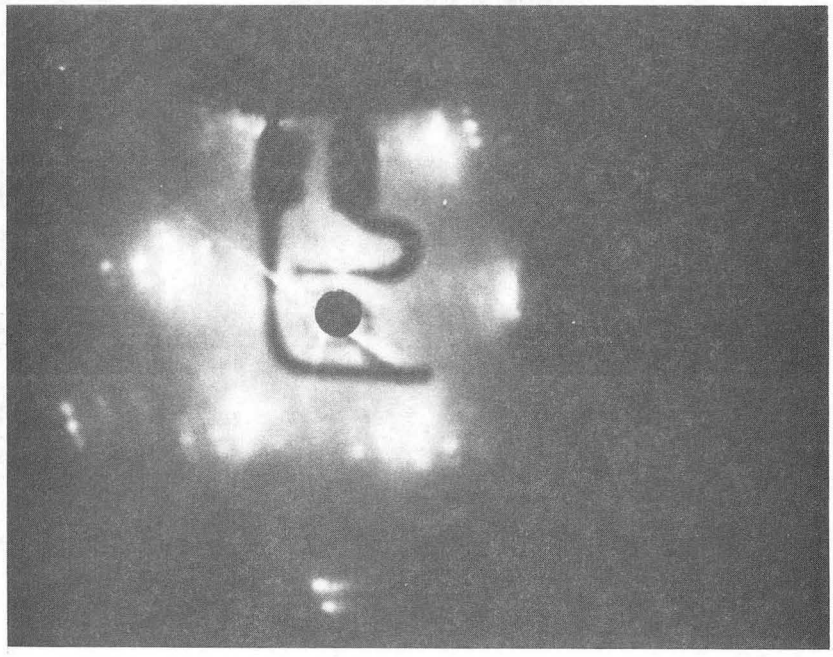

XBB 810-10164

b

Fig.7

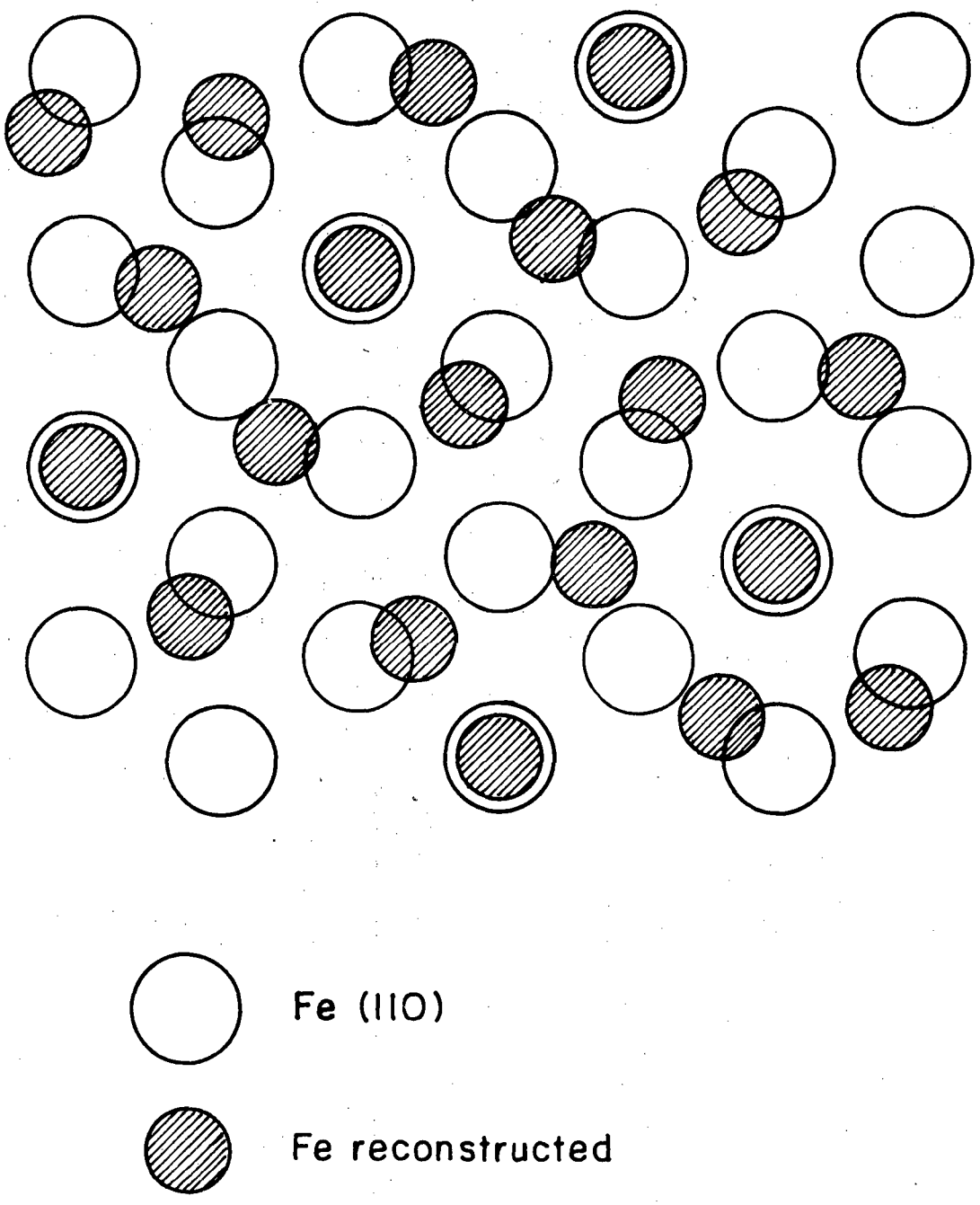

Fig.8

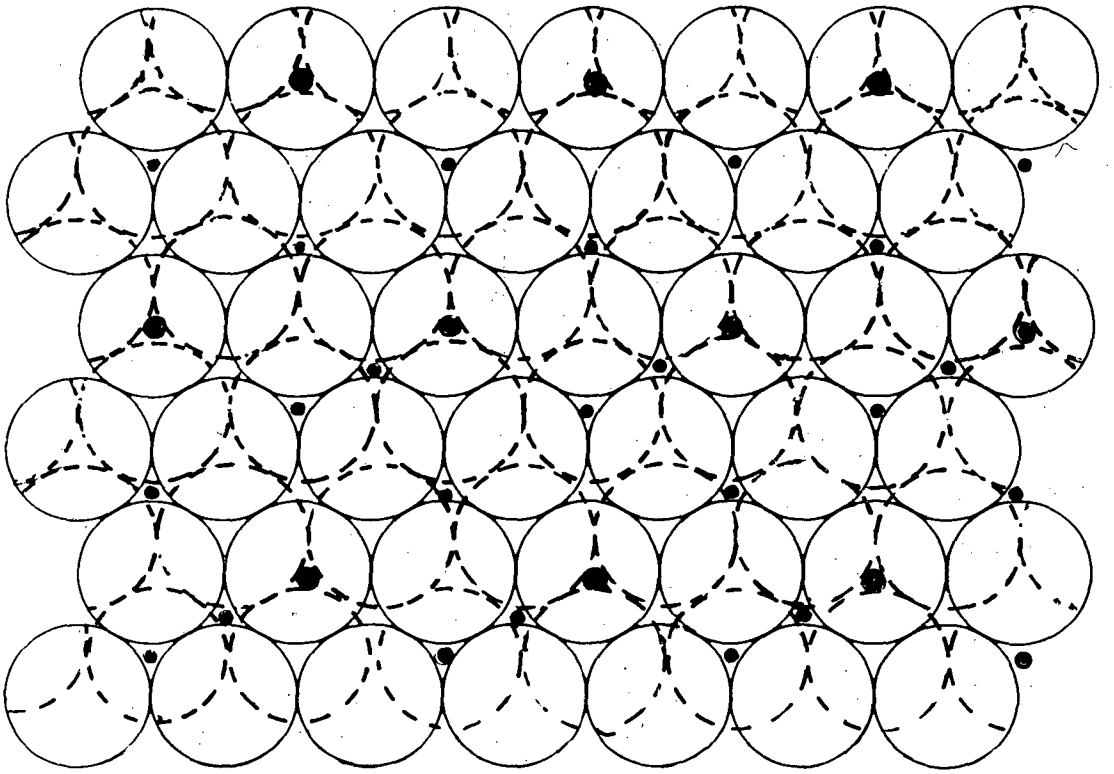

● Tetrahedral site
• Octahedral site

(a)

XBL 8110-6888A

Fig.9

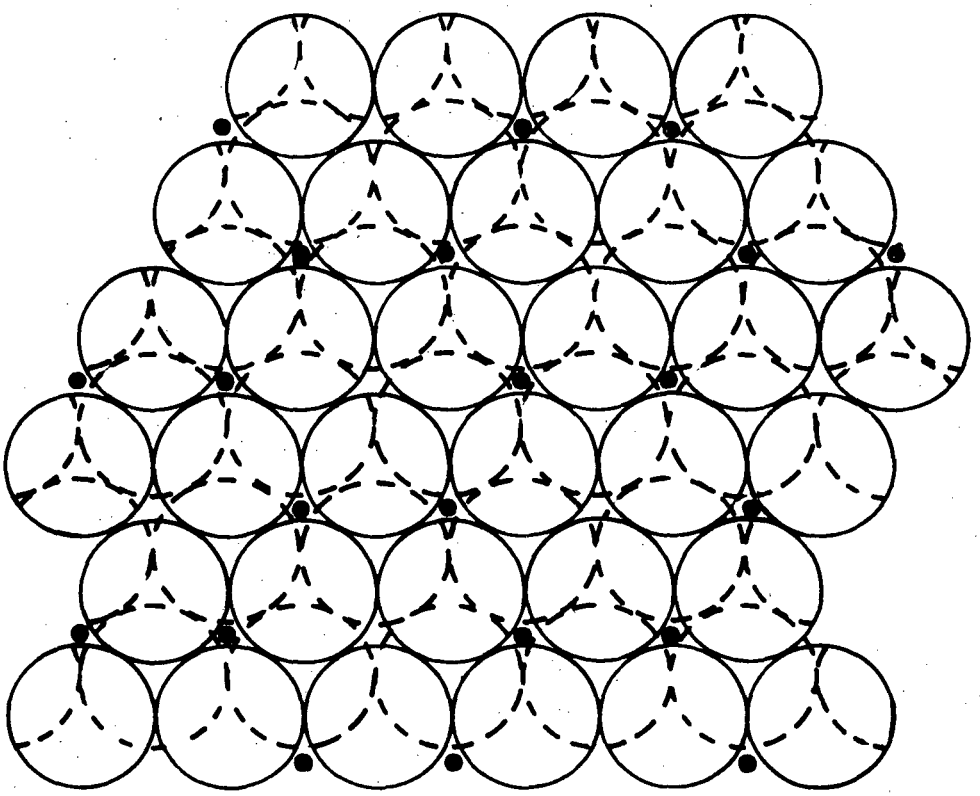

• Octahedral site

(b)

XBL8110-6887

Fig.10

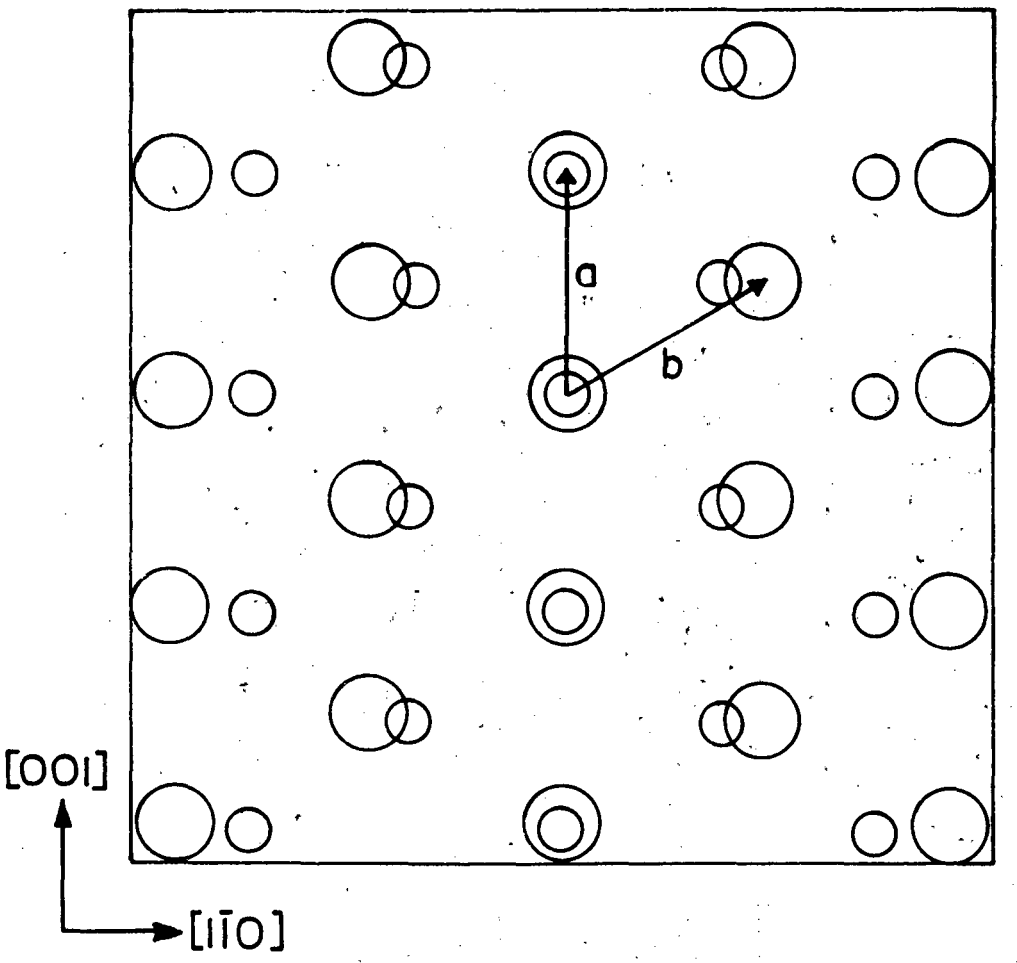
a
b
[001]
[1$\bar{1}$0]
Fe (110) substrate atoms
Fe oxide overlayer
XBL 8110-6888

Fig.11

Table 1. Bulk Oxide Auger Ratios

Bulk Oxide	Treatment	O/Fe
αFe_2O_3 single crystal	oxygen annealed 5×10^{-7} torr O_2, 200°C	4.21 ± .27
α Fe_2O_3 single crystal	UHV annealed 500°C	3.70 ± .15
powder α Fe_2O_3	oxygen annealed 5×10^{-7} torr O_2, 200°C	3.76 ± .15
Fe foil; heavily oxidized (α Fe_2O_3-red)	oxygen annealed .5 Atm O_2; 25-200°C	4.10 ± .17
Fe foil; heavily oxidized (Fe_3O_4-black)	heat αFe_2O_3 500°C UHV (after treatment)	3.75 ± .10
powder Fe_3O_4	UHV annealed 500°C	3.73 ± .19

Table 2. Iron Oxide Epitaxies as a Function of Temperature and Pressure

	$5x10^{-8}$ torr O_2	$5x10^{-7}$ torr O_2	$5x10^{-6}$ torr O_2
25°C	(1x1); 1.48 O/Fe	na	na
100°C	(1x1); 1.72	hexagonal; 3.39	hexagonal; 3.45
200°C	hexagonal; 2.95*	hexagonal; 3.67	hexagonal; 3.76
300°C	reconstructed; 1.32*	hexagonal; 3.61	hexagonal; 3.69
400°C	na	reconstructed; 1.61	hexagonal; 3.76
500°C	reconstructed; 1.06*	reconstructed; 1.73	reconstructed; 1.89

* not to saturation

na - not available

Table 3. Metal-Metal Oxide Epitaxial Arrangement for Some Known Compounds

Metal-metal Oxide	Mismatch	Orientation	Reference
Mo(100)/MoO_2(110)	2-8 %*	Mo[010]/MoO_2[001]	17
Mo(110)/MoO_2(110)	2-8 %*	Mo(110)-->Mo(112) Mo[$\bar{1}$10]/MoO_2[010]	17
W(110)/WO_3(100)	6 %	W[1$\bar{1}$0]/WO_3[$\bar{1}\bar{1}$2]	18,19
W(110)/WO_3(111)	2 %	W[001]/WO_3[110]	19
Fe(100)/Fe_4N(002)	1.3 %	Fe[001]/Fe_4N[110]	20

* metal surface is contracted from bulk value

This report was done with support from the Department of Energy. Any conclusions or opinions expressed in this report represent solely those of the author(s) and not necessarily those of The Regents of the University of California, the Lawrence Berkeley Laboratory or the Department of Energy.

Reference to a company or product name does not imply approval or recommendation of the product by the University of California or the U.S. Department of Energy to the exclusion of others that may be suitable.

TECHNICAL INFORMATION DEPARTMENT
LAWRENCE BERKELEY LABORATORY
UNIVERSITY OF CALIFORNIA
BERKELEY, CALIFORNIA 94720